



A review on biogenic synthesis of ZnS nanoparticles and potential applications

Soma Gorai

Department of Chemistry, Asansol Girls' College, Asansol-713 304, West Bengal, India

E-mail: gorai_soma@rediffmail.com

Manuscript received online 01 December 2020, accepted 29 December 2020

Applications of green chemistry perspective for nanoparticles (NPs) synthesis have gained much attention in recent years mainly to reduce the use of hazardous chemicals and also to eliminate the production of toxic materials. Green bio-based synthesis is an organic molecule mediated technique where nanoparticles are prepared by using naturally occurring reagents such as plant extracts, vitamins, biodegradable polymers, sugars, and microorganisms, etc. The nature of these biological entities influences the structure, size and morphology of synthesized NPs. During the past few decades, researchers have been paying more attention to the synthesis (both physically and chemically) of nontoxic semiconducting zinc sulfide nanoparticles for their diverse applications in different fields. This short review highlighted the alternative eco-friendly and cost-effective bio-based green techniques for the synthesis of ZnS NPs by using various biogenic sources and also focuses on some of the important properties of bio-synthesized ZnS NPs like photocatalytic activity, antimicrobial activity, cytotoxicity and seed germination ability.

Keywords: Green synthesis, zinc sulphide nanoparticles, applications.

Introduction

During the past few decades, nanoscale chalcogenide semiconductors have drawn much attention mainly for their interesting properties. The tiny dimension and high surface area to volume ratio of nanoparticles make their physico-chemical properties unique from those of the bulk materials. For this reason, a wide range of physical and chemical techniques have been developed for the past few years to produce nanoscale materials of different sizes, shapes, and compositions. Now-a-days, to reduce the rate of hazardous chemicals employed in these conventional techniques during the synthesis of these NPs, green bio-based methods using plant parts, fungus, bacteria, and algae or other bio-based molecules (protein, vitamin, molecules etc.) have been adopted¹⁻³. The organic compounds present in these naturally occurring sources act as reducing agents and also as capping agents^{4,5}.

Among the chalcogenide semiconductor NPs, zinc sulphide (ZnS), a large band gap (3.6 eV) semiconductor has been studied more intensively because of its unique properties and potential applications in the biomedical⁶ and opto-

electronic field, such as to prepare biosensors, biocomposites⁷, light-emitting diode (LED), screens, sensors, lasers⁸, or nanocomposites⁹ etc. Due to the non toxic nature of ZnS NPs, it is now utilized for the treatment of waste water where it acts as photocatalyst and degrades several pollutants like organic dyes, *para*-nitrophenol and halogenated derivatives¹⁰⁻¹². For these reasons, various physical and chemical methods have already been reported in the literature^{8,12-16} to fabricate various types of ZnS nanostructures. But in recent years, the eco-friendly and cost-effective green synthesis pathway for synthesizing ZnS NPs has drawn much attention. This review briefly summarizes the recently reported biogenic synthesis of ZnS nanoparticles using various bio-based sources and also focuses on the properties of these green synthesized ZnS NPs like photocatalytic activity, antimicrobial activity, cytotoxicity and seed germination ability.

Green synthesis of ZnS nanoparticles

Various types of plants/plant parts and bio-templated media which are used to synthesize ZnS NPs are discussed below:

Plant source-mediated synthesis:

The plant contains different biomolecules like amino acids, lignins, monosaccharides, polysaccharides, anthraquinones, enzymes, minerals, vitamins, salicylic acids, saponins, sterols etc. The plant phytochemicals with reducing and capping properties are usually responsible for the formation of nanostructured materials^{4,5}. Researchers reported several hypothetical mechanisms^{23,27,48,49} of biosynthesis of nanoparticles using plants/plant parts and to understand the detailed mechanism research is going on.

In recent years, utilization of extracts of different plant parts in the biosynthesis of ZnS NPs has been done by several researchers:

Using plant extract:

Sathishkumar *et al.*¹⁷ biosynthesized ZnS NPs by using *Acalypha indica* (A:ZnS) and *Curcuma longa* plant extract (C:ZnS) in a chemical co-precipitation method. XRD patterns indicated the formation of zinc blende (cubic) structure of ZnS for both cases (Fig. 1).

The uniform particle distribution and size variation of the

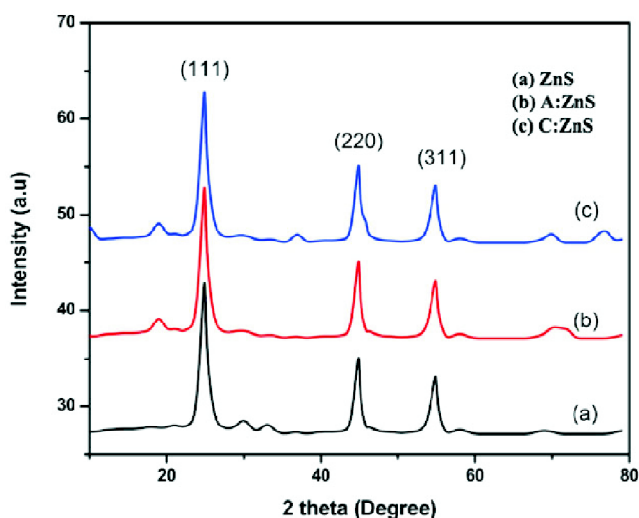


Fig. 1. XRD patterns of (a) ZnS, (b) *Acalypha indica*:ZnS, (c) *Curcuma longa*:ZnS. Reproduced from Ref. [17]. Copyright © 2019, Material Science Research India.

particles in both cases could be observed from SEM images (Fig. 2).

In another study, they¹⁸ utilized methanol extract of

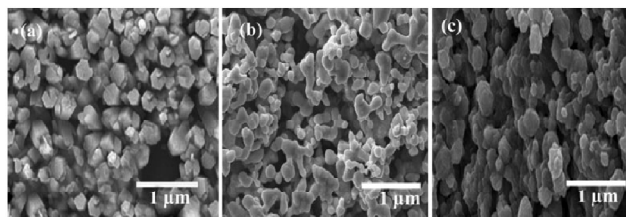


Fig. 2. SEM images of (a) ZnS, (b) *Acalypha indica*:ZnS, (c) *Curcuma longa*:ZnS. Reproduced from Ref. [17]. Copyright © 2019, Material Science Research India.

Phyllanthus niruri plant and found the formation of hexagonal wurtzite structure of ZnS with an average crystallite size ~74 nm. From SEM images ~2 µm size of the surface of hexagonal nanoparticles was found. Further, via a co-precipitation method, employing methanolic extracts of various plants like *Tridax procumbens* (T), *Phyllanthus niruri* (P), and *Syzygium aromaticum* (S) and ZnSO₄.7H₂O, NH₂CSNH₂, 1% NH₃ solution, they made another attempt¹⁹ to synthesize ZnS NPs. A consistent cubic phase of ZnS was observed from XRD spectra. SEM images revealed that the variation of particle size could be done by varying plant extracts.

Using leaf extract:

Using the leaves of the medicinal plant *Abrus precatorius* Biruntha *et al.*²⁰ prepared spherical shaped ZnS NPs. The formation of the crystalline structure of ZnS (cubic form) was confirmed by the XRD analysis. Anand *et al.*²¹ reported the formation of pure and biosynthesized ZnS NPs using *Cucumis sativus* leaf extract. XRD patterns of pure and bio-ZnS NPs indicated zinc blende cubic phase of ZnS. SEM images showed a moderate distribution of the biosynthesized ZnS NPs and the estimated size was found about 38 nm. The leaf extract of *Corymbia citiodora* was utilized by Chen *et al.*²². They found that the extract has reducing ability as well as stabilizing property. The size of uniformly dispersed spherical shaped nanoparticles was found to be 45 nm. The XRD pattern matched well with the zinc blende structure of ZnS (cubic phase). Sathishkumar *et al.*²³ prepared ZnS NPs by using leaf extract of *Lawsonia inermis*. FTIR study revealed the existence of various organic moieties like alkyl, alkyne, aliphatic amine, hydroxyl, aromatic nitro and aldehyde group. From XRD pattern cubic zinc blende structure of ZnS was observed and the calculated average particle size was found

about 4.6 nm. In another experiment²⁶, they employed *Tridax procumbens* leaf extract. Hexagonal wurtzite structure of ZnS NPs (having diameter ~40 nm) was identified from XRD spectrum. Different morphological patterns like hexagonal, spherical and rod shaped particles were observed. *Moringa oleifera* leaf extract was used by Sur *et al.*²⁴. They evaluated the stability of synthesized ZnS NPs by zeta-potential measurement and found that it remained stable for three months. TEM images of the spherical shaped ZnS NPs showed the average diameter of particles was 30 nm. XRD analysis revealed the formation of ZnS having wurtzite structure. They performed a TLC-densitometric study which showed the presence of biomolecules (present in *M. oleifera* leaves) like crypto-chlorogenic acid, isoquercetin and astragalin. The average quantity of the said biomolecules was found 0.0423, 0.0467, and 0.0634% (dry weight), respectively. Alijani *et al.*²⁵ fabricated ZnS NPs by utilizing glycoside, obtained from the leaf extract (aqueous) of *Stevia rebaudiana* (Bertoni). The biomolecule present in the extract performed as a reducing agent. XRD results showed the formation of the cubic phase. Spherical shaped polydispersed NPs having an average particle size of 8.35 nm were observed.

Using fruit peel extract:

Salem *et al.*²⁷ synthesized ZnS NPs using aqueous extract of *Punica granatum* (Pomegranate) peel at ambient temperature and in one single step. It was found that by varying the quantity of peel extract and zinc ion concentration different sizes of particle could be achieved. FTIR spectra showed that the stabilization of ZnS NPs was done via the coordination with -OH, -NH, C=O, C=N. Formation of platelets composed with NPs (av. size 20 nm) was found from SEM image.

Using latex:

Latex-mediated synthesis of ZnS NPs was performed by Hudlikar *et al.*²⁸. They used a solution of 0.3% latex obtained from *Jatropha curcas* L. In their study, latex was used as the precursor of sulphide ions. XRD pattern of the synthesized product showed the cubic phase of ZnS. TEM study revealed the formation of ZnS NPs having particle size of ~10 nm.

Alga mediated synthesis:

Rao *et al.*²⁹ prepared ZnS NPs by employing extract of (cell-free) *Chlamydomonas reinhardtii*. They controlled the

synthesis process by varying pH, temperature and extract amount. FTIR result revealed that cellular proteins might have an important role in the stabilization of ZnS NPs. HR-TEM images indicated that the size of the spherical shaped particles varied within 8–12 nm. XRD analysis showed the characteristics of FCC structure of cubic zinc sulphide.

Fungi mediated synthesis:

Uddandarao *et al.*³⁰ fabricated zinc sulphide quantum dots (Q-dots) using *Aspergillus flavus* (an endophytic fungus). They selected this fungus due to its antioxidant properties. XRD analysis indicated the well crystalline hexagonal phase of biosynthesized ZnS. The presence of spherical shaped particles having diameter within 12–24 nm could be seen from TEM images. Their study (FTIR) demonstrated that proteins can form bond with the NPs via free amine groups and with cysteine residues. This ability of the protein molecules (performing as a capping agent) enhances the stability of the NPs by preventing internal agglomeration. By using the Morris-Weber kinetic model they studied and illustrated the role of biosorption in the preparation of ZnS Q-dots. Suganya *et al.*³¹ biosynthesized ZnS NPs by applying an aqueous extract of edible mushroom, *Pleurotus florida*. XRD result showed the zinc blende structure of ZnS. SEM images revealed the size of the spherical shaped particles varied within a range of 10–20 nm. It was found that with the increase of the concentration of mushroom extract aggregation of NPs decreases. Senapati *et al.*³² employed edible mushroom *Pleurotus ostreatus* for the preparation of NPs. This mushroom possess high amount of proteins, vitamins and amino acids. They used different volumes of mushroom extract to synthesize ZnS NPs. SEM analysis revealed that the agglomerating tendency of the particles decreases with the increase of mushroom extract concentration. The particle size was found to vary from 4.04 to 2.30 nm. Zinc blende structure of ZnS was confirmed by XRD patterns. Mala *et al.*³³ prepared ZnS quantum dots by using *Saccharomyces cerevisiae* MTCC 2918. XRD analysis revealed that the NPs were in the sphalerite phase. From TEM images it was observed that the particle size varied within 30–40 nm.

Bacteria mediated synthesis:

At room temperature and atmospheric pressure through

a single-step process Gong *et al.*³⁴ synthesized ZnS NPs by using *Desulfovibrio desulfuricans*. They deduced that ZnS NPs were formed when Zn^{2+} entered into the bacterial cells and combined with S^{2-} by a dissimilatory sulfate reduction. After completion of accumulation of ZnS NPs in the membranes, these (ZnS NPs) were ultimately expelled extracellularly. XRD pattern and EDX analysis confirmed the formation of ZnS. HR-TEM analysis (Fig. 3) showed that the size of the spherical shaped particles varied within the range of 2–8 nm depending on the reaction time.

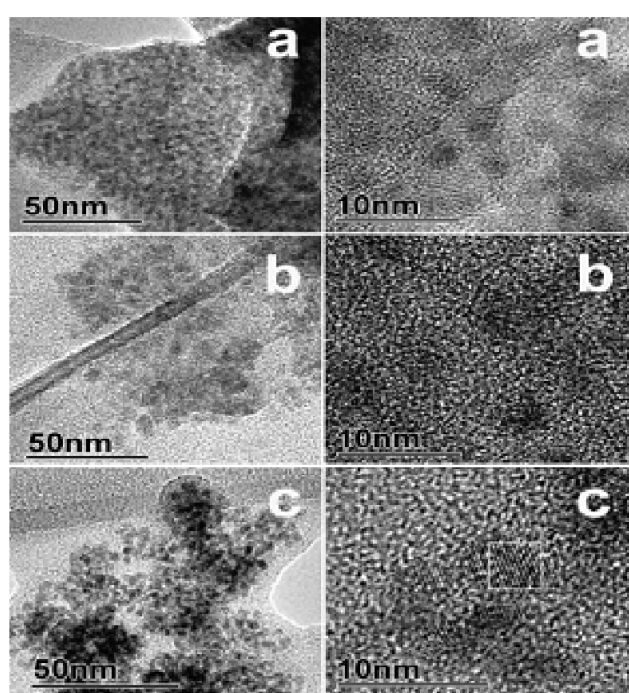


Fig. 3. HR-TEM micrographs of prepared ZnS particles (Bacteria mediated) (a) HR-TEM image after 24 h, (b) HR-TEM image after 48 h, (c) HR-TEM image after 96 h. Reproduced from Ref. [34]. Copyright © 2018, Taylor & Francis (Inorganic and Nano-Metal Chemistry).

Malarkodi *et al.*³⁵ reported an extracellular synthesis of ZnS NPs by using *Klebsiella pneumoniae* bacteria. Incubation of the mixture of bacterial supernatant and $ZnSO_4$ was done for 24 h at 35°C. *K. pneumoniae* detoxified the $ZnSO_4$ and produced the nanosized ZnS particles. The formation of ZnS NPs was identified from surface plasmon spectra and also from XRD measurement. They demonstrated from FTIR results that the proteins present in the bacterial cell performed

as a reducing agent and controlled the synthesis of ZnS nanoparticles in the colloidal solution. TEM analysis showed that spherical shaped particles having ~65 nm of diameter were formed. In another experiment³⁹ they utilized *Serratia nematodiphila*. They isolated this sulfur-reducing bacterium from a chemical company effluent. TEM study revealed the formation of spherical shaped NPs having 80 nm diameter. Hazra *et al.*³⁶ used rhamnolipids for capping and stabilizing ZnS NPs. They isolated rhamnolipids by the certain procedures from *P. aeruginosa* BS01. The biosurfactant concentration was maintained sufficiently higher than the Zn^{2+} concentration for immediate arresting of the particles at a smaller size. XRD analysis confirmed the formation of crystalline ZnS NPs. TEM images showed the presence of 10–15 nm particles having spherical shape. Narayanan *et al.*³⁷ also used rhamnolipids for capping ZnS NPs. Rhamnolipids was synthesized microbially and extracted from *P. aeruginosa*. It was found that around the neutral pH agglomeration of particles occurred. Hence, they performed the reaction at pH 10 using 1 M NaOH. The capped NPs were found stable and water soluble. FTIR study revealed that a complex was formed between rhamnolipid and Zn ions. TEM images showed the presence of spherical shaped particles (5–10 nm). Bai *et al.*³⁸ developed a bio-based technique utilizing immobilized *Rhodobacter sphaeroides* for the preparation of zinc sulphide NPs. Cubic phase of ZnS was revealed from XRD analysis. TEM image of ZnS NPs indicated that spherical shaped particles having size of ~12 nm were formed. It was seen that according to the culture time the particle size of NPs was varied from 4 to 105 nm. They explained that the increase of particle size occurred due to the agglomeration of smaller particles into larger ones (“nucleation effect”). Xiao *et al.*⁴⁰ bio fabricated ZnS NPs by using *Shewanella oneidensis* MR-1 bacteria. XRD data showed that the cubic phase of ZnS was formed. The shape of the biosynthesized ZnS NPs was spherical (~5 nm) and the particles were observed to remain aggregated mainly in the medium and cell surface of *S. oneidensis* MR-1.

Using other bio-based sources:

Chanu *et al.*⁴¹ synthesized ZnS NPs by hydrothermal method where amino acid, L-histidine was used as the capping agent. Various parameters like reaction time, temperature, pH and precursor ratio control the shape and size of the

synthesized ZnS NPs. They found to form 5 nm of spherical particle when the reaction temperature was fixed at 120°C for 3 h. A facile hydrothermal route was adopted by Dong *et al.*⁴² where amino acid, L-histidine was used as the capping agent. It was observed that the reaction parameters like temperature and time influenced the variation of particle size. The mean diameters of ZnS nanosphere were found to vary within 203.1 to 268.5 nm depending on reaction temperature and time. XRD study confirmed the formation of wurtzite phase of ZnS. Ayodhya *et al.*⁴³ described a hydrothermal method for the fabrication of zinc sulphide NPs (particle size 20 nm) by utilizing Bovine Serum Albumin (BSA). At 120°C and 15 lbs. pressure they treated Zn(CH₃COO)₂·2H₂O, Na₂S and 1% w/v BSA for 60 min. The formation and stability of ZnS NPs were studied using EDX, XRD, FTIR, UV-Vis diffuse reflectance spectrum (DRS) and zeta potential measurement. FTIR study showed the existence of interactions between Bovine serum albumin and Zn²⁺ ions. They suggested that BSA helps to inhibit the agglomeration of the NPs. In a wet chemical method, Tiwari *et al.*⁴⁴ prepared ZnS NPs by using a carbohydrate-based matrix, hypromellose (hydroxypropyl methylcellulose) (HPMC). XRD spectra indicated a zinc blende structure. From thermogravimetric analysis it was suggested that at 700°C, polymer attached to the

surface decomposed. TEM images showed that ZnS NPs were well dispersed into the HPMC-matrix which indicated that HPMC played the role of a stabilizing agent during the biosynthesis of ZnS. Deb *et al.*⁴⁵ followed a wet chemical route to prepare ZnS nanostructures by using starch as a green capping agent under nitrogen environment. XRD spectra confirmed the formation of cubic phase (zinc blende) ZnS NPs.

HR-TEM images exhibited the average particle size of the spherical-shaped particle varied within the range of 4.35–5.5 nm. Senapati U.S. *et al.*⁴⁶ used glucose for the preparation of ZnS NPs. FTIR study showed that -C-O and -OH groups of glucose could bind with ZnS NPs. The experiment also revealed that nearly spherical shaped particles were formed having an average particle size 5.83 nm. XRD analysis revealed that the green synthesized ZnS has a cubic structure. Abbas *et al.*⁴⁷ also prepared ZnS NPs by microwave assisted irradiation method using glucose. It acts as a capping agent and also as a stabilizer. From FTIR study they suggested that ZnS NPs were encapsulated by glucose. XRD pattern identified the cubic structure of zinc sulphide having ~3 nm of size.

The aforesaid bio-based media which are used to synthesize ZnS NPs are summarized in Table 1.

Table 1. Various sources and morphological studies of ZnS-NPs

Green parts	Name of the source	Precursor material used	Morphology and size	Ref.
Plant	<i>Acalypha indica</i>	Zinc sulphate,	Spherical, 17.8 nm	17
	<i>Curcuma longa</i>	thiourea	Spherical, 16.9 nm	17
Plant	<i>Phyllanthus niruri</i>	Zinc sulphate	Hexagonal, average size ~74 nm	18
Plant	<i>Phyllanthus niruri</i>	Zinc sulphate,	Spherical, 203.1 nm	19
	<i>Syzygium aromaticum</i>	thiourea	Spherical, 218.4 nm	19
	<i>Tridax procumbens</i>		Spherical, 165.9 nm	19
Leaf	<i>Abrus precatorius</i>	Zinc sulphate	Spherical	20
Leaf	<i>Cucumis sativus</i>	Zinc sulphate	Spherical, 38 nm	21
Leaf	<i>Corymbia citiodora</i>	Zinc sulphate	Spherical, 45 nm	22
Leaf	<i>Lawsonia inermis</i>	Zinc sulphate	Cuboidal, 4.6 nm	23
Leaf	<i>Moringa oleifera</i>	Zinc chloride, sodium sulphide	Spherical, ~30 nm	24
Leaf	<i>Stevia rebaudiana</i> Bertoni	Zinc nitrate, sodium sulphide	Spherical, 8.35 nm	25
Leaf	<i>Tridax procumbens</i>	Zinc sulphate	Hexagonal, spherical, and rod shaped, ~40 nm	26
Fruit peel	<i>Punica granatum</i>	Zinc acetate, sodium sulphide	Platelets, 20 nm	27

Table-1 (contd.)

Latex	<i>Jatropha curcas</i> L.	Zinc acetate	Spherical, 10 nm	28
Cell free extract of Alga	<i>Chlamydomonas reinhardtii</i>	Zinc sulphate	Spherical, 8–12 nm	29
Fungi	<i>Aspergillus flavus</i>	Zinc sulphate	12–24 nm	30
Fungi	<i>Pleurotus florida</i>	Zinc chloride, sodium sulphide	Spherical, 10–20 nm	31
Fungi (edible mashroom)	<i>Pleurotus ostreatus</i>	Zinc chloride, sodium sulphide	Spherical, 4.04 to 2.30 nm	32
Yeast biomass	<i>Saccharomyces cerevisiae</i> MTCC 2918	Zinc sulphate	Spherical, 30–40 nm	33
Bacterial cells	<i>Desulfovibrio desulfuricans</i>	Zinc acetate	Spherical, 2–8 nm	34
Bacterial cells	<i>Klebsiella pneumoniae</i>	Zinc sulphate	Spherical, average diameter 65 nm	35
Rhamnolipid	<i>Pseudomonas aeruginosa</i>	Zinc chloride, sodium sulphide	Spherical, 3–10 nm	36
Rhamnolipid	<i>Pseudomonas aeruginosa</i>	Zinc chloride, sodium sulphide	Spherical, 5–10 nm	37
Bacterial cell	<i>Rhodobacter sphaeroides</i>	Zinc sulphate	Spherical, 12 nm	38
Bacterial cell	<i>Serratia nematodiphila</i>	Zinc sulphate	Spherical, 80 nm	39
Bacterial cell	<i>Shewanella oneidensis</i> MR-1	Zinc sulphate, sodium thiosulphate	Spherical, 5 nm	40
Amino acid	L-Histidine	Zinc nitrate, sodium sulphide	Spherical, 5 nm	41
Amino acid	L-Histidine	Zinc acetate, thioacetamide	Spherical, 203.1–268.5 nm	42
Protein	Bovine Serum Albumin (BSA)	Zinc acetate and sodium sulphide	Agglomerated particle, <10 nm	43
Carbohydrate	Hypromellose (hydroxypropyl methylcellulose)	Zinc acetate and sodium sulphide	Spherical	44
Carbohydrate	Starch	Zinc acetate and thiourea	Spherical, 4.35–5.5 nm	45
Glucose	Glucose	Zinc nitrate and sodium sulphide	Spherical, 5.83 nm	46
Glucose	Glucose	Zinc nitrate and sodium sulphide	3 nm	47

Applications

Several studies revealed that biosynthesized ZnS has many important applications (Fig. 4).

These are discussed briefly in the following sections:

Photocatalytic property:

Chen *et al.*²² examined the photocatalytic property of synthesized ZnS NPs towards Methylene blue (MB) dye under UV light irradiation and noticed that 96% degradation of the dye occurred within 2 h. The small particle size and excellent dispersibility of green-synthesized ZnS NPs help to exhibit enhanced photocatalytic activity in comparison with chemically prepared ZnS nanoparticles. Sathishkumar *et al.*¹⁹ also studied the photocatalytic activity of ZnS NPs (synthesized using *Syzygium aromaticum* extract) towards MB dye and Methyl orange (MO) dye in aqueous solution under UV

light irradiation and observed that ZnS NPs (1.0 mg) exhibited excellent photocatalytic degradation of MB dye (81%) and MO dye (99%). They also found that the rate of organic pollutant dye degradation depends on the photocatalyst percentage and irradiation time. Hazra *et al.*³⁶ studied the photocatalytic degradation of direct brown MR in presence of synthesized ZnS NPs spectrophotometrically in a batch reactor. The optimum dosage of ZnS NPs (Rhamnolipid synthesized) was found 120.0 mg L⁻¹. The maximum efficiency of degradation was observed in alkaline pH of 11. A maximum dye degradation of 94% was found under UV irradiation for 180 min at optimum conditions using ZnS NPs. Xiao *et al.*⁴⁰ observed a good degree of photodegradation efficiency of ZnS NPs (prepared using *Shewanella oneidensis* MR-1) towards rhodamine B (RhB). Their study indicated that photogenerated holes might be responsible for the photo-

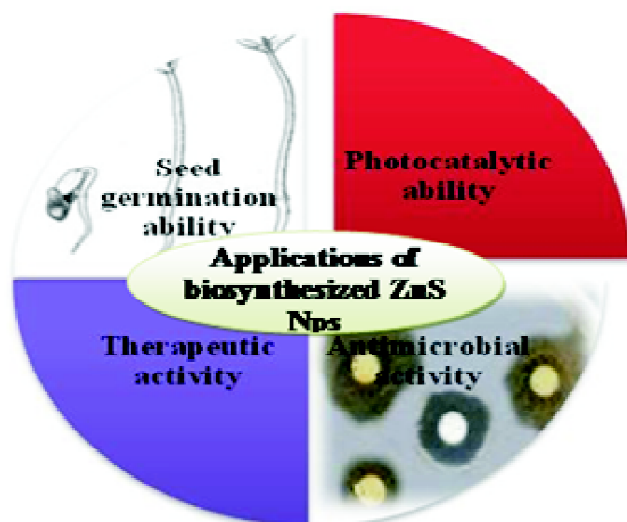


Fig. 4. Pictorial representation of the applications of biosynthesized ZnS.

catalytic decolorization of RhB. Ayodhya *et al.*⁴³ also evaluated the photocatalytic activity of BSA capped ZnS nanoparticles towards the degradation of RhB dye under sunlight irradiation. They observed that the above procedure obeys pseudo-first order kinetics. Experimental results revealed that the biosynthesized ZnS nanoparticles have better photocatalytic efficiency than photolysis, this might occur because of the surface capping of BSA molecules. They also studied the fluorescence quenching and binding of ZnS NPs with crystal violet (CV). Results of the various calculated parameters like binding constants, binding sites, and bimolecular quenching constants indicated that in reaction medium CV and ZnS nanoparticles formed stable complex.

Antimicrobial activity:

Malarkodi *et al.*³⁵ successfully demonstrated the bactericidal and fungicidal activity of biosynthesized ZnS NPs against *Streptococcus* sp., *Staphylococcus aureus*, *Lactobacillus* sp., and *Candida albicans*, respectively by disc diffusion method with zone of inhibition (ZOI) on the agar plate. It was observed that the growth rate of *Lactobacillus* sp., *Staphylococcus aureus*, *Candida albicans*, and *Streptococcus* sp. reduced with the increase of ZnS NPs amount. In another experiment, Malarkodi *et al.*³⁹ examined the antibacterial ability of ZnS NPs on *Bacillus subtilis* (Gram-positive) and *Klebsiella planticola* (Gram-negative) and found that the highest ZOI was 21.66 ± 0.66 and 22.66 ± 1.454 mm, re-

spectively, for 200 μL concentration. It was explained that different nature of the cell wall of two types of bacteria made them able to respond differently towards ZnS NPs. Kumar *et al.*¹⁸ also found that green synthesized (*Phyllanthus niruri* plant mediated) zinc sulphide nanoparticles exhibited very good antimicrobial activity on several microorganisms like Gram-positive, Gram-negative bacteria and fungus cultures. They used an *in vitro* disc diffusion technique for analysing the antimicrobial activity of zinc sulphide and found that the highest zone of inhibition was obtained in *Candida albicans* fungus culture and lowest inhibition zone was observed in *Bacillus subtilis* bacteria followed by *Aspergillus niger* fungus at a concentration of 60 μL . In another experiment¹⁹, they observed that biosynthesized ZnS NPs showed a high zone of inhibition at different concentrations against all tested microorganisms compared to pure ZnS NPs. It was also noticed that the S:ZnS NPs (using *Syzygium aromaticum*) exhibited excellent antimicrobial activity against all tested microorganisms compared to other ZnS NPs. Further, they¹⁷ studied the antimicrobial activity of ZnS NPs synthesized by using *Acalypha indica*, *Curcuma longa* plant extract against different human pathogens. The maximum zone of inhibition was obtained for plant extract mediated ZnS compared to pure ZnS NPs and explained that this might be due to the influence of smaller crystal size (of biosynthesized ZnS NPs than pure ZnS NPs) and presence of biomolecule from plant extracts. Antimicrobial activity of ZnS NPs was also investigated by Abbas *et al.*⁴⁷ against MDR pathogenic bacteria, *Pseudomonas aeruginosa*, and *Staphylococcus aureus*. The MIC tests demonstrated that 37.5 $\mu\text{g}/\text{ml}$ of ZnS NPs had the best antibacterial activity against both *P. aeruginosa* and *S. aureus*. Sathishkumar *et al.*²³ tested the antimicrobial property of leaf extract (*Lawsonia inermis*) on several microorganisms. It was observed that at concentrations 30 μL only *S. aureus*, *E. coli* and *P. aeruginosa* were inhibited and at concentrations 40 μL and 50 μL , the maximum inhibition was observed against *P. aeruginosa* and *B. subtilis* followed by *S. typhi*. In another study, they²⁶ found that ZnS NPs synthesized by using *Tridax procumbens* have a very good ZOI in the various microorganisms like *S. aureus*, *B. subtilis* and *E. coli*, *P. aeruginosa* and *C. albicans*, *A. niger* (fungus). The highest ZOI was found in *P. aeruginosa* (22 mm) in 60 μL concentration and the minimum was noticed in *A. niger* (15 mm).

Cytotoxicity study:

Alijani *et al.*²⁵ determined the cytotoxic effect of ZnS NPs on human cancer cell line (MCF-7) by utilizing colorimetric assay and made a comparison with the untreated control group as normal cell lines. When ZnS NPs and Stevia extract were applied on human cancer cell line they found IC₅₀ values of 400 and 2000 µg/ml, respectively. Their study revealed that synthesized NPs prevented the cancer cell line growth in a dose-dependent manner. Biruntha *et al.*²⁰ conducted the toxicity tests for a period 14 days with synthesized ZnS NPs on the earthworm *E. eugeniae* and found zero mortality rate.

Seed germination study:

To evaluate the biofertilization potential of NPs, Suganya *et al.*³¹ conducted an *in vitro* seed germination study with green gram (*V. radiata*) using different concentrations of biosynthesized ZnS NPs. The experiment revealed that under controlled conditions ZnS NPs positively influence seed germination and the early growth of green gram. Salem *et al.*²⁷ studied the effect of ZnS NPs on germinations and seminal roots. It was noticed that the percentage of germination, root length and number of seminal routes of cucumber seed were significantly influenced by the different concentrations of ZnS NPs (100–1000 ppm). Application of 400 ppm ZnS NPs to cucumber seeds showed highly favorable growth promoting effects on cucumber growth.

Conclusions

The development of eco-friendly technology for the synthesis of NPs is a vital step in the area of nanotechnology. Now-a-days, it is a new and emerging area of research. The present review summarizes different bio-based green techniques for the synthesis of ZnS NPs by using various biogenic sources and also focuses on some of the properties of bio-synthesized ZnS NPs. This database shows the potential of bio-based materials for the synthesis of ZnS NPs from which researchers may able to plan for their future research work on the said fields.

References

1. L. Castro, M. L. Blázquez, J. Á. Muñoz, F. G. González and A. Ballester, *IET Nanobiotechnol.*, 2013, **7**, 109.
2. S. Gorai, *J. Mater. Environ. Sci.*, 2018, **9**, 2894.

3. P. Vani, N. Manikandan and G. Vinitha, *Asian J. Pharm. Clinic. Res.*, 2017, **April**, 337.
4. T. Bhuyan, K. Mishra, M. Khanuja, R. Prasad and A. Varma, *Mater. Sci. Semicond. Process*, 2015, **32**, 55.
5. N. C. Sharma, S. V. Sahi, S. Nath, J. G. Parsons, J. L. Gardea-Torresdey and P. Tarasankar, *Environ. Sci. Technol.*, 2007, **41**, 5137.
6. G. R. Amir, S. Fatahian and N. Kianpour, *Current Sci.*, 2014, **10**, 796.
7. P. Wu, Y. He, H. F. Wang and X. P. Yan, *Anal. Chem.*, 2010, **82**, 1427.
8. H. Ali, S. Karim, M. A. Rafiq, K. Maaz, A. U. Rahman, A. Nisar and M. Ahmad, *J. Alloys Compd.*, 2014, **612**, 64.
9. K. Dutta, S. Manna and S. K. De, *Synth. Met.*, 2009, **159**, 315.
10. Y. Wada, T. Kitamura, S. Yanagida and H. Yin, *Chem. Commun.*, 1998, **24**, 2683.
11. J. S. Hu, L. L. Ren, Y. G. Guo, H. P. Liang, A. M. Cao, L. J. Wan and C. L. Bai, *Angew. Chem.*, 2005, **117**, 1295.
12. Y. Chen, R.-H. Yin and Q.-S. Wu, *J. Nanomater.*, 2012, **2012**, 1.
13. Y. Zhao, J. M. Hong and J. J. Zhu, *J. Cryst. Growth*, 2004, **270**, 438.
14. Y. Li, X. He and M. Cao, *Mater. Res. Bull.*, 2008, **43**, 3100.
15. Y. Hao, G. Meng, Z. L. Wang, C. Ye and L. Zhang, *Nano Lett.*, 2006, **6**, 1650.
16. D. Lin, H. Wu, R. Zhang and W. Pan, *J. Am. Ceram. Soc.*, 2007, **90**, 3664.
17. M. Sathish Kumar, S. Manickam and V. Muthusamy, *Mater. Sci. Res. India*, 2019, **16**, 174.
18. M. SathishKumar, S. Manickam and V. Muthusamy., *Int. J. Chem. Sci.*, 2017, **15**, 123.
19. M. Sathish Kumar, S. Manickam, V. Muthusamy and R. Thangaraj, *J. Nanostruct.*, 2018, **8**, 107.
20. M. Biruntha, J. Archana, K. Kavitha, B. K. Selvi, J. A. J. Paul, R. Balachandar, M. Saravanan and N. Karmegam, *Bio Nano Sci.*, 2019, **1**.
21. B. Anand, A. Muthuvel, V. Mohana, P. Selvarani and B. Lakshmi, *Int. J. S. Res. Sci. Tech.*, 2018, **4**, 817.
22. J. Chen, B. Hu and J. Zhi, *Physica E: Low-dimen. Syst. Nanostruct.*, 2016, **79**, 103.
23. M. Sathishkumar, N. P. Subiraminiam and M. Sasikumar, *Nehru E-J.*, 2017, **5**, 17.
24. U. K. Sur and B. Ankamwar, *RSC Adv.*, 2016, **6**, 95611.
25. H. Q. Alijani, S. Pourseyedi, M. T.-Mahani and M. Khatami, *J. Molecular Str.*, 2019, **1175**, 214.
26. M. Sathishkumar, M. Saroja, M. Venkatachalam, G. Parthasarathy and A. T. Rajamanickam, *Orient. J. Chem.*, 2017, **33**, 903.
27. N. M. Salem, L. S. Albanna and A. M. Awwad, *J. Agric. Bio. Sci.*, 2017, **12**, 167.

28. M. Hudlikar, S. Joglekar, M. Dhaygude and K. Kodam, *J. Nanopart. Res.*, 2012, **14**, 865.
29. M. D. Rao and G. Pennathur, *Green Processing and Synthesis*, 2016, **5**, 379.
30. P. Uddandarao and R. Mohan, *Materi. Sci. Eng. (B)*, 2016, **207**, 26.
31. P. Suganya and P. U. Mahalingam, *IOSR J. Appl. Chem.*, 2017, **10**, 37.
32. U. S. Senapati and D. Sarkar, *Indian J. Phys.*, 2014, **88**, 557.
33. J. G. S. Mala and C. Rose, *J. Biotechnol.*, 2014, **170**, 73.
34. J. Gong, X. Song, Y. Gao, S. Gong, Y. Wang and J. Han, *Inorg. Nano-Metal Chem.*, 2018, **0**, 1.
35. C. Malarkodi, S. Rajeshkumar, K. Paulkumar, M. Vanaja, G. Gnanajobitha and G. Annadurai, *Bioinorg. Chem. Appl.*, **2014**, Article ID 347167, 2014, 1.
36. C. Hazra, D. Kundu, A. Chaudhari and T. Jana, *J. Chem. Technol. Biotechnol.*, 2012, **88**, 1039.
37. J. Narayanan, R. Ramji, H. Sahu and P. Gautam, *IET Nanobiotechnol.*, 2010, **4**, 29.
38. H.-J. Bai, Z.-M. Zhang and J. Gong, *Biotechnol. Lett.*, 2006, **28**, 113.
39. C. Malarkodi and G. Annadurai, *Appl. Nanosci.*, 2013, **3**, 389.
40. X. Xiao, X.-B. Ma, H. Yuan, P.-C. Liu, Y.-B. Lei, H. Xu, D.-L. Du, J.-F. Sun and Y.-J. Feng, *J. Hazard. Mater.*, 2015, **288**, 134.
41. T. I. Chanu, D. Samanta, A. Tiwari and S. Chatterjee, *Appl. Surf. Sci.*, 2017, **391**, 548.
42. F. Dong, Y. Guo, J. Zhang, Y. Li, L. Yang, Q. Fang, H. Fang and K. Jiang, *Mater. Lett.*, 2013, **97**, 59.
43. D. Ayodhya and G. Veerabhadram, *J. Fluoresc.*, 2016, **26**, 2165.
44. A. Tiwari, S. A. Khan, R. S. Kher and S. J. Dhoble, *Luminescence*, 2014, **29**, 637.
45. S. Deb, P. K. Kalita and P. Datta, *Inter. J. Nanosci.*, 2018, **17**, 1760032.
46. U. S. Senapati, D. K. Jha and D. Sarkar, *Res. J. Physical Sci.*, 2013, **1**, 1.
47. N. K. Abbas, I. Al-Ogaidi, M. Alsalmami and S. Talla, *Global. J. BioSc., Biotech.*, 2017, **6**, 677.
48. J. Osuntokun, D. C. Onwudiwe and E. E. Ebenso, *J. Clust. Sci.*, 2017, **28**, 1883.
49. J. C. Selvakumari, M. Ahila, M. Malligavathy and D. P. Padiyan, *Int. J. Miner. Metallur. Mater.*, 2017, **24**, 1043.